



Offshore Code Comparison Collaboration within IEA Wind Annex XXIII: Phase III Results Regarding Tripod Support Structure Modeling

Conference Paper
NREL/CP-500-44810
January 2009

J. Nichols and T. Camp
Garrad Hassan & Partners Limited, United Kingdom

J. Jonkman and S. Butterfield
National Renewable Energy Laboratory, United States

T. Larsen and A. Hansen
Risø National Laboratory, Denmark

J. Azcona, A. Martinez, and X. Munduate
National Renewable Energies Center, Spain

F. Vorpahl and S. Kleinhansl
*Fraunhofer Center for Wind Energy and Maritime Engineering,
Germany*

M. Kohlmeier, T. Kossel, and C. Böker
Leibniz University of Hannover, Germany

D. Kaufer
University of Stuttgart, Germany

*Presented at the 47th Annual Aerospace Sciences Meeting
Orlando, Florida
January 5 – 8, 2009*



NREL is operated for DOE by the Alliance for Sustainable Energy, LLC

Contract No. DE-AC36-08-GO28308



NOTICE

The submitted manuscript has been offered by an employee of the Alliance for Sustainable Energy, LLC (ASE), a contractor of the US Government under Contract No. DE-AC36-08-GO28308. Accordingly, the US Government and ASE retain a nonexclusive royalty-free license to publish or reproduce the published form of this contribution, or allow others to do so, for US Government purposes.

This report was prepared as an account of work sponsored by an agency of the United States government. Neither the United States government nor any agency thereof, nor any of their employees, makes any warranty, express or implied, or assumes any legal liability or responsibility for the accuracy, completeness, or usefulness of any information, apparatus, product, or process disclosed, or represents that its use would not infringe privately owned rights. Reference herein to any specific commercial product, process, or service by trade name, trademark, manufacturer, or otherwise does not necessarily constitute or imply its endorsement, recommendation, or favoring by the United States government or any agency thereof. The views and opinions of authors expressed herein do not necessarily state or reflect those of the United States government or any agency thereof.

Available electronically at <http://www.osti.gov/bridge>

Available for a processing fee to U.S. Department of Energy and its contractors, in paper, from:

U.S. Department of Energy
Office of Scientific and Technical Information
P.O. Box 62
Oak Ridge, TN 37831-0062
phone: 865.576.8401
fax: 865.576.5728
email: <mailto:reports@adonis.osti.gov>

Available for sale to the public, in paper, from:

U.S. Department of Commerce
National Technical Information Service
5285 Port Royal Road
Springfield, VA 22161
phone: 800.553.6847
fax: 703.605.6900
email: orders@ntis.fedworld.gov
online ordering: <http://www.ntis.gov/ordering.htm>



Offshore Code Comparison Collaboration within IEA Wind Annex XXIII: Phase III Results Regarding Tripod Support Structure Modeling

J. Nichols and T. Camp
Garrad Hassan & Partners Limited (GH)
United Kingdom, St Vincent's Works, Silverthorne Lane, Bristol BS2 0QD
Telephone: +44 (0) 117 972 9900 Fax: +44 (0) 117 972 9901
E-mail: james.nichols@garradhassan.com

J. Jonkman and S. Butterfield¹
National Renewable Energy Laboratory (NREL), United States of America

T. Larsen and A. Hansen
Risø National Laboratory for Sustainable Energy, Technical University of Denmark

J. Azcona, A. Martinez, and X. Munduate
National Renewable Energies Center (CENER), Spain

F. Vorpahl and S. Kleinhansl
Fraunhofer Center for Wind Energy and Maritime Engineering (CWMT), Germany

M. Kohlmeier, T. Kossel, and C. Böker
Leibniz University of Hannover, Germany

and

D. Kaufer
Endowed Chair of Wind Energy, University of Stuttgart, Germany

Offshore wind turbines are designed and analyzed using comprehensive simulation codes that account for the coupled dynamics of the wind inflow, aerodynamics, elasticity, and controls of the wind turbine, along with the incident waves, sea current, hydrodynamics, and foundation dynamics of the support structure. This paper presents an overview and describes the latest findings of the code-to-code verification activities of the Offshore Code Comparison Collaboration, which operates under Subtask 2 of the International Energy Agency Wind Annex XXIII. In the latest phase of the project, a variety of project participants used an assortment of codes to model the coupled dynamic response of a 5-MW wind turbine installed on a tripod substructure in 45 m of water. The code predictions from a set of load case simulations—each selected to test different features of the models—were compared side by side. The comparisons have resulted in a more thorough understanding of the modeling techniques and better knowledge of when various approximations are not valid. Importantly, the lessons learned from this exercise have been used to improve the codes of the participants, hence improving the standard of offshore wind turbine modeling.

¹ Employees of the Alliance for Sustainable Energy, LLC, under Contract No. DE-AC36-08GO28308 with the U.S. Dept. of Energy have authored this work. The United States Government retains and the publisher, by accepting the article for publication, acknowledges that the United States Government retains a non-exclusive, paid-up, irrevocable, worldwide license to publish or reproduce the published form of this work, or allow others to do so, for United States Government purposes.

I. Introduction

The vast offshore wind resource represents a potential to use wind turbines installed offshore to power much of the world. Design standardization is difficult, however, because offshore sites vary significantly in water depth, soil type, and wind and wave severity. To ensure that offshore wind turbine installations are cost effective, the application of a variety of support structure types is required. These types include fixed-bottom monopiles, gravity bases, and space-frames—such as tripods, tetrapods, and lattice frames (e.g., “jackets”)—and floating structures. In this context, the offshore wind industry faces many new design challenges.

Wind turbines are designed and analyzed using comprehensive simulation tools (i.e., design codes) capable of predicting the coupled dynamic response and the extreme and fatigue loads of the system. Land-based wind turbine analysis relies on the use of aero-servo-elastic codes, which incorporate wind-inflow, aerodynamic (aero), control system (servo), and structural-dynamic (elastic) models in the time domain in a fully coupled (integrated) simulation environment. In recent years, some of these codes have been expanded to include the additional dynamics pertinent to offshore installations, including the incident waves, sea current, hydrodynamics, and foundation dynamics of the support structure¹. The sophistication of these aero-hydro-servo-elastic codes, and the limited data available with which to validate them, underscore the need to verify the codes to ensure their accuracy and correctness. The Offshore Code Comparison Collaboration (OC3), which operates under Subtask 2 of the International Energy Agency (IEA) Wind Annex XXIII, was established to meet this need.

The OC3 project is performed through technical exchange among a group of international participants who come from universities, research institutions, and industry across the United States of America (U.S.), Germany, Denmark, the United Kingdom (UK), Spain, the Netherlands, Norway, Sweden, and Korea. In this paper, specifically, results are presented from participants who come from Risø National Laboratory of Denmark; Garrad Hassan & Partners Limited (GH) of the UK; the National Renewable Energies Center (CENER) of Spain; and the Fraunhofer Center for Wind Energy and Maritime Engineering (CWMT), the Leibniz University of Hannover (LUH) and the Endowed Chair of Wind Energy at the University of Stuttgart (SWE), all from Germany.

II. Overview of the OC3 Project

A. Phase III in Relation to Other Phases

The simulation of offshore wind turbines under combined stochastic aerodynamic and hydrodynamic loading is very complex. The benchmarking task therefore requires a sophisticated approach that facilitates the identification of sources of modeling discrepancies introduced by differing theories and model implementations in the various codes. This is possible only by (1) meticulously controlling all of the inputs to the codes, and (2) carefully applying a stepwise verification procedure where model complexity is increased in each step.

To encompass the variety of support structures required for cost effectiveness at varying offshore sites, different types of support structures (for the same wind turbine) are investigated in separate phases of the OC3 project:

- In Phase I, the NREL offshore 5-MW wind turbine is installed on a monopile with a rigid foundation in 20 m of water.
- In Phase II, the foundation of the monopile from Phase I is made flexible by applying different models to represent the soil-pile interactions.
- In Phase III, the water depth is changed to 45 m and the monopile is swapped with a tripod substructure, which is one of the common space frame concepts proposed for offshore installations in water of intermediate depth.
- In Phase IV, the wind turbine is installed on a floating platform in deep water.

The fundamental set of inputs to the codes controlled within OC3 relates to the specifications of the wind turbine. The OC3 project uses the publicly available specifications of the 5-MW baseline wind turbine developed by NREL, which is a representative utility-scale multimegawatt turbine that has also been adopted as the reference model for the integrated European Union UpWind research program. This wind turbine is a conventional three-bladed upwind variable-speed variable blade-pitch-to-feather-controlled turbine. The specifications consist of detailed definitions of the rotor aerodynamic properties; blade, drive train, nacelle, and tower structural properties; and generator-torque and blade-pitch control system properties, the latter of which was provided to all OC3 participants in the form of a dynamic link library. Reference 2 lists the specifications of the NREL offshore 5-MW baseline wind turbine in detail. The hydrodynamic and elastic properties of the varying offshore support structures used in the project are also controlled, and are discussed later. Furthermore, the turbulent full-field wind inflow and regular and irregular wave kinematics are model inputs controlled within the OC3 project. Risø generated the turbulent wind velocity datasets and GH generated the wave kinematics datasets; these datasets were then provided to all other participants. This approach eliminates any possible differences brought about by dissimilar turbulence models, wave theories, or stochastic realizations.

An important part of the comparison is a stepwise process that allows the origin of differences between code predictions to be discovered. The first phase introduced the turbine with a rigid foundation. Various combinations of wave and wind input were introduced with the rotor and tower being rigid or flexible, disentangling the contributions from wind and wave applied loads and dynamic response. Finally, the turbine was made operational so that the effect of the control system could be evaluated.

The second phase introduced the effects of a flexible foundation. Phase III examines the effects of wave loading on a more complicated support structure in deeper water. Emphasis within the OC3 project is placed on the verification of the offshore support structure dynamics as part of the dynamics of the complete system. This emphasis is a feature that distinguishes the OC3 projects from other wind turbine code-to-code verification exercises that have been performed in the past. Nevertheless, it was important to test the aerodynamic models separately so that modeling differences resulting from the aerodynamics could be identified. This identification is important because the aerodynamic models are known to be a routine source of differences in wind turbine code-to-code comparisons.

The OC3 project started in January 2005 and is scheduled to be completed in spring 2009. Since the start of the project, the reference 5-MW wind turbine, including the control system, has been developed; the wind and wave datasets have been generated; the simulations and code-to-code comparisons of Phases I, II, and III have been completed; and Phase IV has been initiated. A discussion of the wind and wave dataset generation and a description of Phases I and II and their results are presented in detail in Ref. 3 and Ref. 4, respectively. This paper describes Phase III and discusses its results. Phase IV will be presented in future papers.

B. Simulations To Be Performed for Phase III

In Phase III a set of three load case simulations has been defined for the NREL offshore 5-MW wind turbine² installed on a tripod substructure with rigid foundations in 45 m of water (Figure 1). The specifications of each load case simulation are summarized in Table 1. Additionally, an Eigenanalysis is used to verify the full-system structural dynamics.

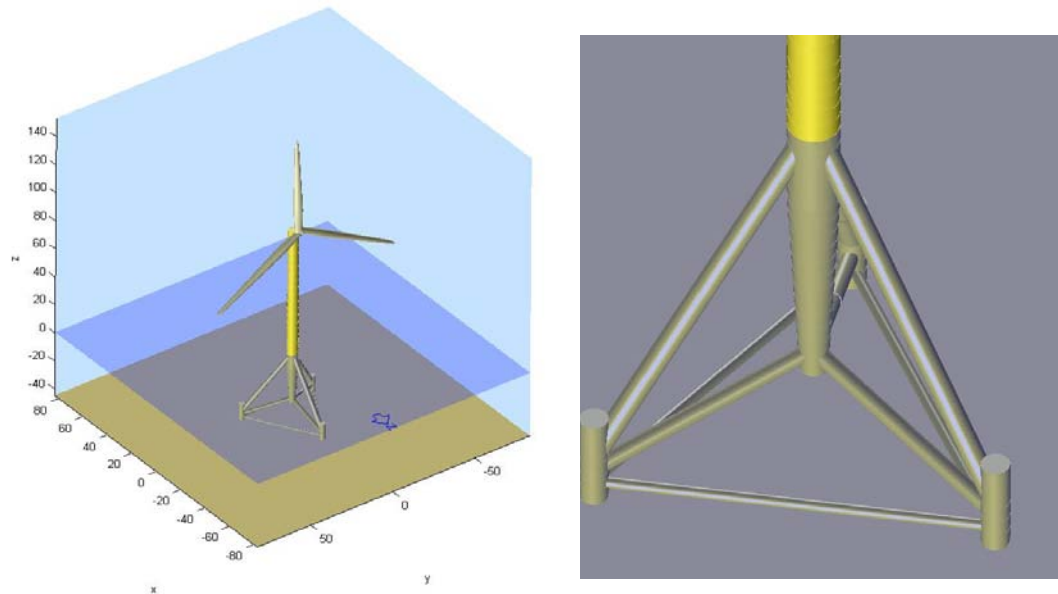


Figure 1. NREL 5MW wind turbine on tripod support structure

The load case identifiers in Table 1 correspond to the identifiers used by the equivalent simulations from Phase I (see Ref. 3), which employed a monopile with a rigid foundation model. In Phase III, though, it was not necessary to independently test the aerodynamic, hydrodynamic, and aero-servo-elastic models—as was done in Phase I—because these models were identical between Phases I and III. Fewer combinations of wind and wave conditions were also needed to test the tripod substructure models in Phase III. Consequently, the set of simulations from Phase III is much smaller than the set used in Phase I; as a result, the load case identifiers are not sequential.

Load Case	Flexible Subsystems	Wind Conditions	Wave Conditions
2.6	None	None: air density = 0	NWH: Stream Function (Dean), H = 8m, T = 10s
2.7	None	None: air density = 0	None: water density = 0
4.3	Substructure, Tower	None: air density = 0	NWH: Stream Function (Dean), H = 8m, T = 10s
5.1	Substructure, Tower, Drivetrain, Blades	Steady, uniform, no shear: $V_{hub} = 8\text{m/s}$	NWH: Stream Function (Dean), H = 8m, T = 10s
		V_{hub} – hub-height wind speed averaged over 10 minutes	H – individual wave height T – individual wave period

Table 1. Load case definition for Phase III

The tripod support structure is shown in Figure 1. The tripod is a good test for the offshore structure modeling capabilities of codes because it incorporates a number of features not present in conventional monopile support structures:

- There is no overall axial symmetry; especially there is asymmetry between forward and backward and between fore-aft motion and side-side motion.
- Different numbers of members connect at various nodes.
- The central member is significantly tapered.
- Members are at varying angles to the vertical.

For each load case simulation, 57 model output sensors were initially analyzed. In addition to the 47 sensors analyzed in Phase I for the rotor, drive train, nacelle tower, and environment (again, see Ref. 3), 35 more outputs were analyzed in Phase III. These included more tower loads, as well as water particle velocities and accelerations, to better understand the differences between the results of the different codes.

C. Review of Phase I and Phase II Results

Before discussing Phase III, it is important to summarize the key findings from Phases I and II because many of the modeling differences that led to code-to-code discrepancies in Phase I have followed through into subsequent phases. Though the code-to-code comparisons in Phase I agree very well in general, the key reasons for the differences that remained were as follows^{3,4}:

- The modal-based codes (FAST, Bladed, and FLEX5) predict slightly different second and higher coupled eigenmodes than those predicted by the higher fidelity multibody- and FEM-based codes (ADAMS and HAWC2). Differences in the dynamic response and energy content are therefore to be expected in the higher frequency range.
- The codes that rely on full-field wind that is supplied in polar coordinates (FLEX5) predict smoother aerodynamic loads (and thus smaller load deviations and smaller damage equivalent loads) than codes that rely on rectangular coordinates (FAST, Bladed, ADAMS, and HAWC2). This follows from the method in which the wind datasets were generated. To ensure that all participants used the same wind inflow, the full-field wind datasets were generated in rectangular coordinates and subsequently interpolated to polar coordinates for the codes that needed it. This cause for differences was mitigated as much as possible by using a fine spatial resolution (32×32 points across the rotor disk).
- The differences between the codes relating to the implementation of aerodynamic induction, tower interference, hub and tip loss, and dynamic stall models—and whether or not the aerodynamic loads are applied in the deflected or undeflected blade state—attribute to variations in the mean values of several key wind turbine loads (e.g., blade-root bending moments, rotor torque, and rotor thrust).
- The blade-pitch controller compensates somewhat for variations that might have been caused between codes that do (ADAMS and HAWC2) and do not (FAST, Bladed, and FLEX5) have blade-twist degrees of freedom (DOFs).
- Differing model discretizations for the aerodynamic and hydrodynamic loads lead to differences between the code predictions. This is most apparent in the substructure loads that depend strongly on the discretization of hydrodynamic loads near the free surface.
- Even though every effort has been made to standardize model inputs, user error still happens. It often takes several revisions before the model is developed and run as intended. It is also possible in some instances that errors still remain and account for otherwise unexplainable modeling differences.

Phase II was based on Phase I with the addition of three different foundation models. Phase III does not have any foundation DOF modeled; therefore, the results from Phase II, when differing from those from Phase I, have less bearing on this report. However, there was further evidence of some codes producing more excitation in the second tower frequencies when elements pass through the wave surface. The agreement between different codes was better when all the DOFs of the turbine were enabled and it was operating. This is because the substructure loads are heavily influenced by the aerodynamics and the higher frequency discrepancies are damped out.

D. Wider Objectives of the Project

To test the newly developed codes, the main activities of the OC3 project are (1) discussing modeling strategies, (2) developing a suite of benchmark models and simulations, (3) running the simulations and processing the simulation results, and (4) comparing the results in a side-to-side fashion. But these activities fall under the much broader objectives of

- Assessing the accuracy and reliability of results obtained by simulations to establish confidence in the predictive capabilities of the codes
- Training new analysts how to run and apply the codes correctly
- Identifying and verifying the capabilities and limitations of implemented theories
- Investigating and refining applied analysis methodologies
- Identifying further research and development needs.

Such verification work, in the past, has led to dramatic improvements in model accuracy as the code-to-code comparisons and lessons learned have helped identify deficiencies and needed improvements in existing codes. These results are important because the advancement of the offshore wind industry is closely tied to the development and accuracy of dynamics models.

Most of the aero-hydro-servo-elastic codes that have been developed for modeling the dynamic response of offshore wind turbines are tested within OC3. The existing modeling capabilities of the simulation tools used by (and for some, developed by) each participant have been discussed in papers on previous phases of the project^{3,4}.

III. Phase III Modeling

Phase III has stretched the abilities of the codes that have been mainly developed to model simple monopile towers. HAWC2 models the wind turbine in the multibody representation; ADCoS models the wind turbine as a nonlinear finite element system with beam elements used for the support structure; FAST and GH Bladed both use a modal representation. In the past couple of years GH Bladed has released a multimember support structure module that allows the modes of complicated structures to be modeled. CENER has used the NASTRAN code to model the wave interaction with a tripod model and a Guyan technique⁵ to use these results as input to FAST. Risø has modeled the tripod structure with its multibody wind turbine code, HAWC2. CWMT has developed a model of the NREL turbine using the nonlinear, finite element code ADCoS, with hydrodynamic forces applied as nodal forces derived from ASAS. The University of Hannover has modeled the tripod structure in Ansys and used WaveLoads to apply the forces from the sea state. The University of Stuttgart has used a modal based wind turbine code, Flex, coupled with Poseidon, a finite element tool.

Overall, the Phase III results have been encouraging. Modal-based and multibody codes have produced similar results. There have been many stages of comparison, as modeling complex offshore support structures is a relatively new development in wind turbine design. With each comparison, the results have converged.

A. Full-System Eigenanalysis

Figure 2 gives the lowest 13 natural frequencies calculated for the stationary—but fully flexible—offshore wind turbine atop a tripod support structure. The designation of “pitch” and “yaw” in the asymmetric flapwise and edgewise blade modes identifies coupling of the blade motions with the nacelle-pitching and nacelle-yawing motions, respectively.

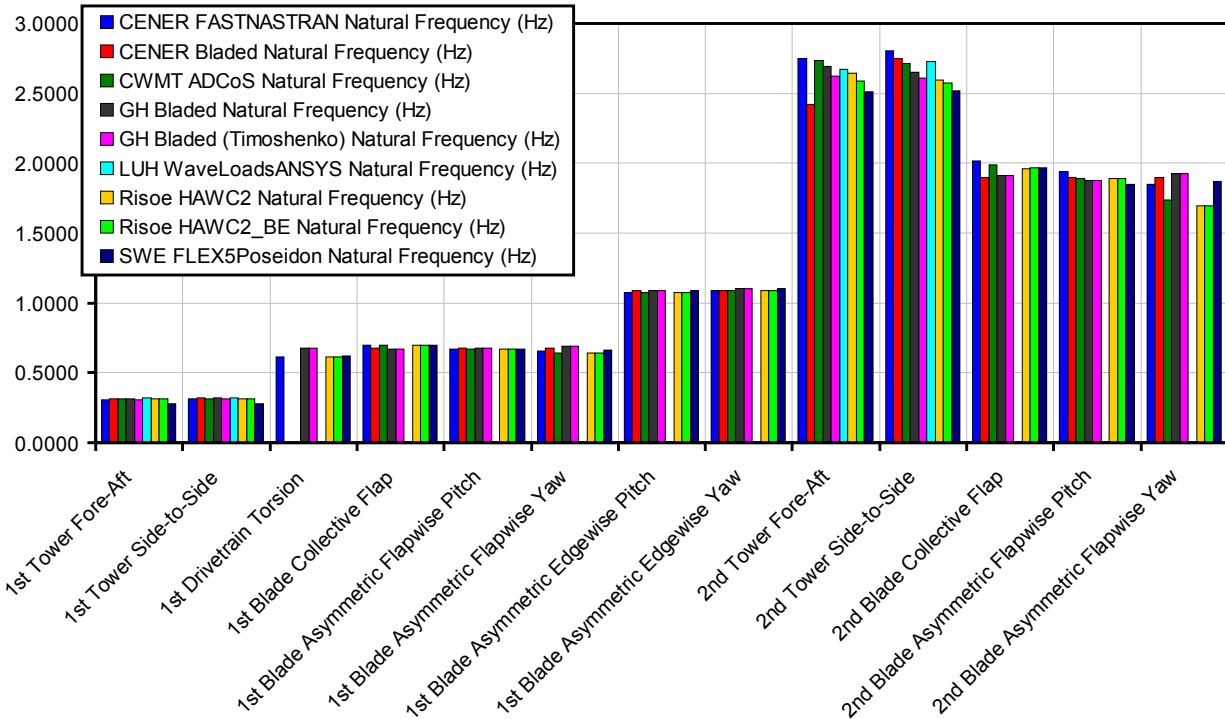


Figure 2. Eigenanalysis of the NREL 5-MW turbine with tripod support structure

The tripod support structure is stiffer than the monopile used in Phase I, increasing the tower natural frequencies by 15%–20%. The increased stiffness of the tower has little effect on the natural frequencies of the blades; however, the drive train frequency is increased slightly. The discrepancy in second tower fore-aft modes is partially due to the

coupling between rotor and tower modes. In particular, the Bladed version used by CENER is a previous version in which there was no coupling term between the tower nodding motion and the rotor out-of-plane motion. The lower values of the second blade asymmetric flapwise yaw mode found by Risø with HAWC2 and CWMT with ADCoS are due to the inclusion of the tower torsional mode. For this mode, the vertical blade remains stationary, whereas the other two blades move out of phase with each other. If the support structure can twist, the effective stiffness of this mode is reduced and therefore the frequency decreases.

B. Specific Problems in Phase III that Have Been Resolved

The participants noted that there are no models of wave run-up and run-down or slap and slam loading implemented in codes. As far as we are aware, no model is implemented in a code for offshore structures.

One difference that could not be overcome between the multibody codes and modal codes has been the issue of modal damping. For the HAWC2, Rayleigh damping has been used and the damping for a mode calculated from a sum over the members. It was not possible to reduce the Rayleigh damping coefficient sufficiently to produce the same modal damping that was used in Bladed and FAST without causing numerical difficulties.

1. Discretization of wave loads near the sea surface

One of the first problems that was observed in Phase III was the appearance of stepwise jumps in the member loads near the free surface of the sea. These were reduced to negligible levels by discretizing the hydrodynamic loads more finely near the sea surface. Figure 3 shows the axial force in the upwind leg of the tripod with both a coarse and a fine discretization.

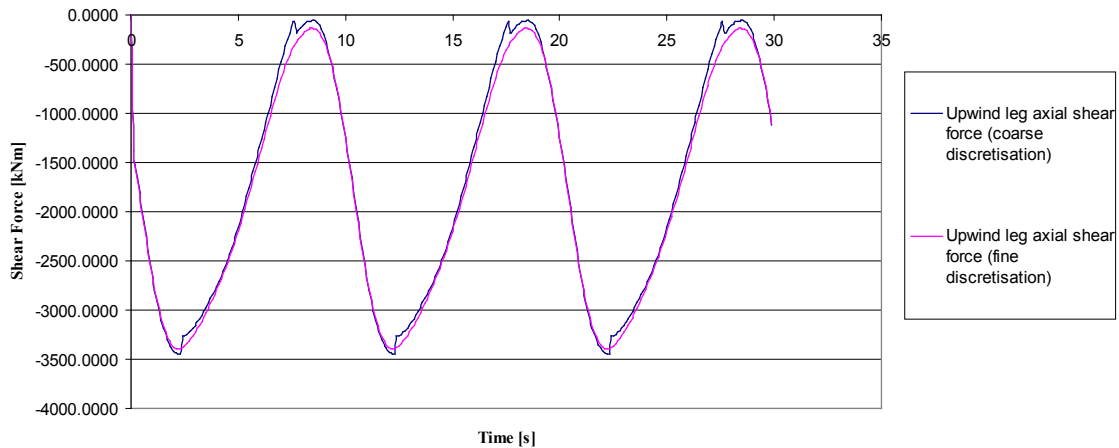


Figure 3. Effect of increasing resolution of hydrodynamic loads near the free surface

2. Discretization of tapered members

The discretization of the tapered, central element of the tripod had a large effect on the loads. Buoyancy and inertial Morison's forces per unit length both depend on the square of the diameter of the member, so having too long a length between members can cause a large error in the total force. Figure 4 shows the fore-aft shear force in the central member when the tapered member is divided into 6 sections and the difference when the member is divided into 17 sections.

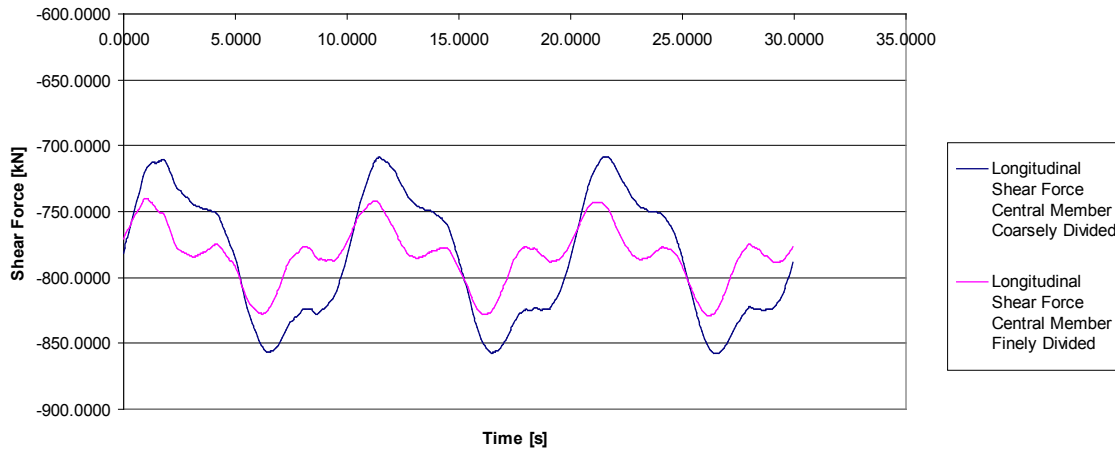


Figure 4. Effect of increasing number of members making up the central, tapered member

3. Overlap of tripod members

Another large effect is caused by the overlapping of members at joints. Figure 5 shows an example of the overlapping region close to the mean sea level in the tripod. For the large diameter members of the tripod configuration, significant surface areas and volumes are duplicated, distorting the overall level of wave and buoyancy loading. The intersecting members will also have an influence on the mass of the tripod. This later influence does not show up in the code to code comparison, however, as all the participants made the assumption that the overlapping sections of mass are negligible.

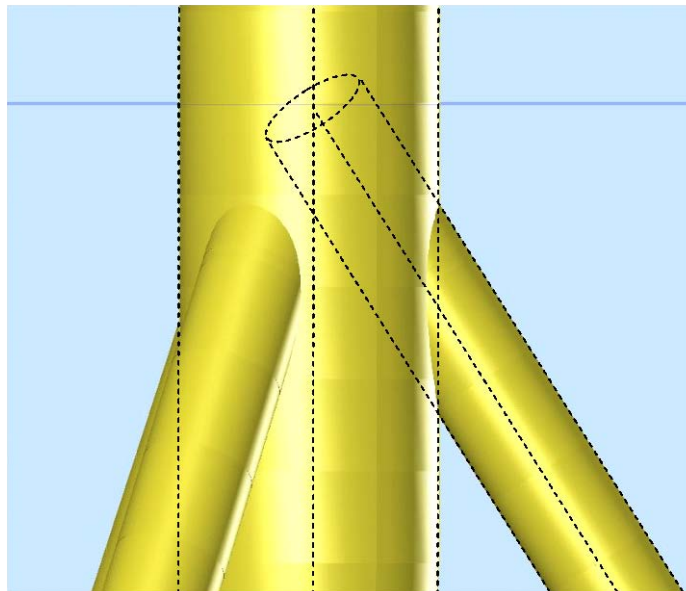


Figure 5. Schematic of overlapping region between two members

In all, 18 sections overlap, neglecting the sections in which the overlap is between three members in total. The difference between assuming the members intersect at the defined nodes and removing these overlapping sections is 159 m³, or 8% of the total volume below sea level. Therefore, it has a significant effect on the buoyancy calculation as well as the applied Morison's equation forces.

4. Shear deflection in tripod members

For a long time it was not possible to get a good match in results between the codes. To find the reason, we performed a simplified study of the turbine mounted on the tripod (Section IV-A). The simplest case of this was a static analysis with gravity as the only external load. Even for this simple case there were major discrepancies. Actually the HAWC2 results were deviating from the rest of the results. The reason for the discrepancies was the difference in beam model, which was demonstrated by CWMT using different kinds of beam elements in ANSYS. The importance can be seen in Figure 6, where only the static loads from gravity are shown. In HAWC2 a Timoshenko beam is used as default, where all other codes use Bernoulli-Euler beams. Because all beams are thin and slender, the Bernoulli-Euler approach should be sufficient, but because the beams are attached rigidly in all ends of the tripod structure, the shear effect is much more important than originally assumed. To verify these findings, we delivered HAWC2 results delivered using both Timoshenko beams and the same beams neglecting the shear effects by increasing the form factor by 10⁴. Also, the Bladed results were delivered using both Timoshenko beams and Bernoulli-Euler beams, also showing the same results. In Figure 6 the axial compression force in the vertical center member of the tripod is shown. The results are different with a factor of 1.9. However, this is the part of the structure where the difference is largest. This difference in solution will also be present for external loads transmitted from the turbine to tripod as, for example, aerodynamic loads.

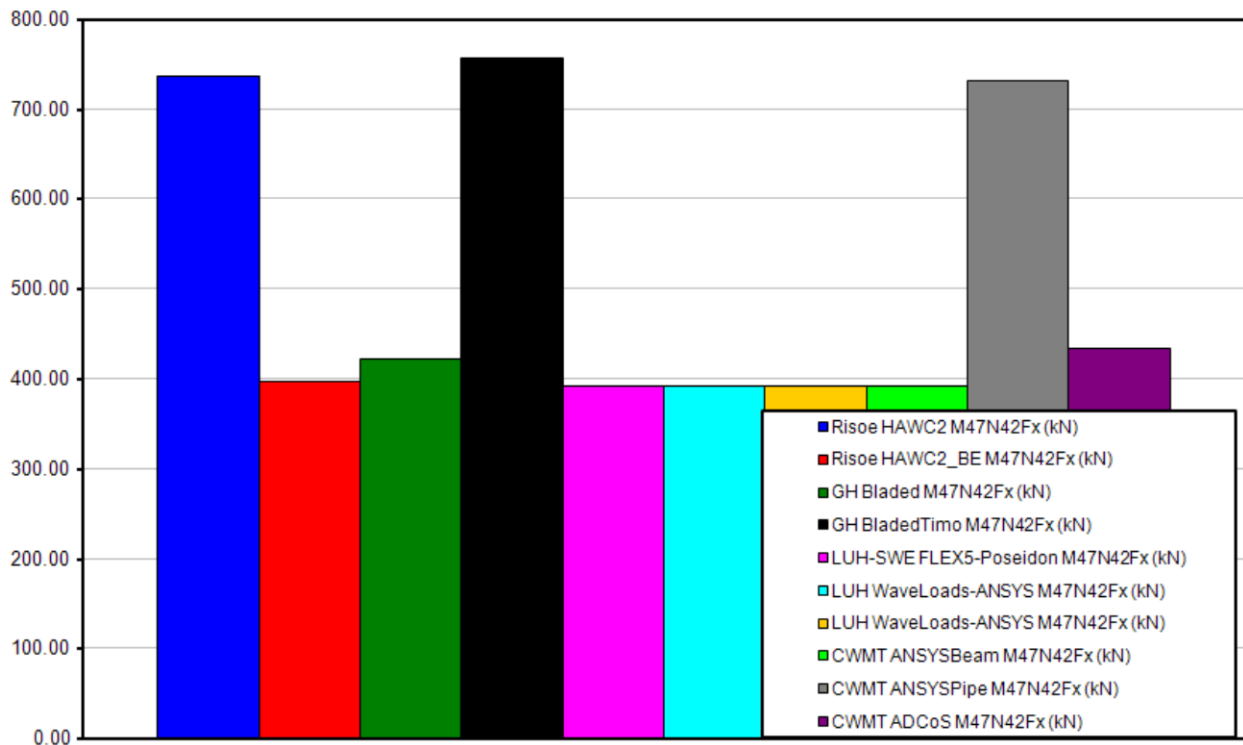


Figure 6. Axial force in the vertical center beam of the tripod. A clear difference can be seen between codes using Bernoulli-Euler or Timoshenko beams. The HAWC2, Bladed, and ANSYNS, results are submitted in two versions with either Timoshenko beams or Bernoulli-Euler beams.

IV. Loading Simulations

Six locations were chosen for output to best capture the influence of the waves on the structure and are shown in Figure 7. The first station, 2 m above the mean sea level, illustrates the effects of wave kinematics near the top of the wave; the second station is at the intersection of three slanted legs and one central member; the third is a tapered member; the fourth and fifth are in the center of the two upwind slanted members; and the final is the load at the start of the foundation.

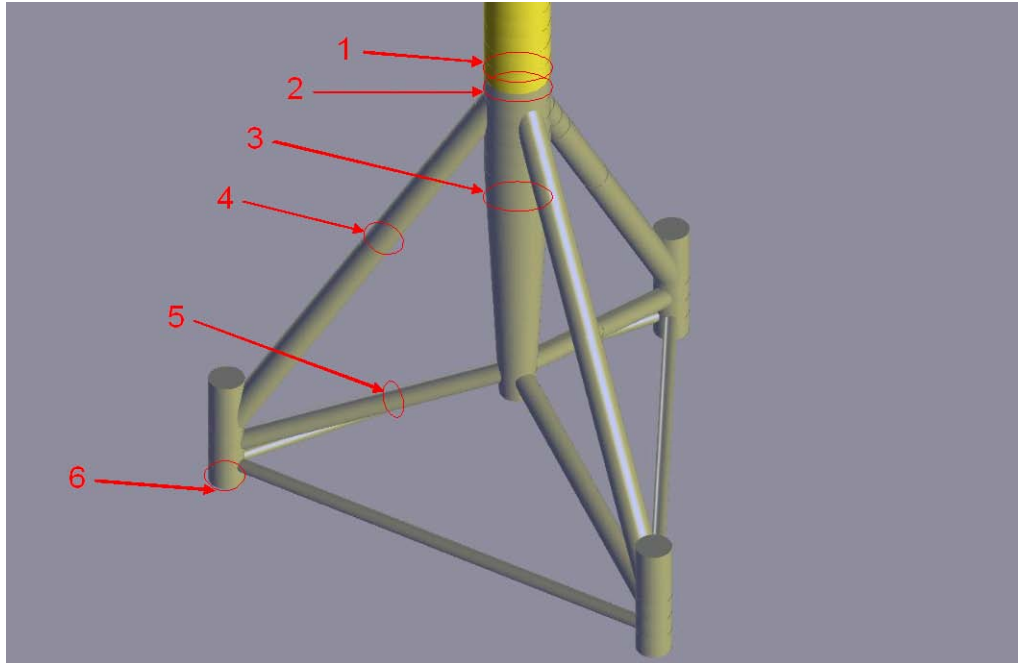


Figure 7. Locations for load output

Six participants contributed time domain simulations to this phase of the project with six different code combinations being used. The legend that will be used for the results of these simulations is shown in Figure 8.

— CENER FASTNASTRAN	— CENER Bladed
— CWMT ADCoS	— GH Bladed
— GH Bladed (Timoshenko)	— LUH WaveLoads.ANSYS
— Risoe HAWC2	— Risoe HAWC2_BE

Figure 8. Legend for loads

A. Load Case 2.7: Loads in the Structure out of the Water

The tripod structure presents new challenges in wind turbine modeling. For instance, it is not a tree-like structure and has to support dynamic loads through axial forces rather than bending moments. Therefore, it was decided to compare the loads on the structure caused solely by gravity, without complications caused by buoyancy and wave loads, to iron out differences in the structural modeling.

Because of the difference in results between the two beam definitions (Section 3B4), the results are presented in two groups; one for the Euler-Bernoulli formulation and one for the Timoshenko formulation. GH Bladed, SWE Flex Poseidon, CWMT ADCoS, LUH Waveloads Ansys, Risø HAWC2_BE and CWMT ANSYS Beam all used the Euler-Bernoulli element. Risø HAWC2, CWMT ANSYS Pipe, and GH Bladed (Timoshenko) used the Timoshenko element. The overall spread is also shown to illustrate which loads are most affected by the beam formulation. As shown in Tables 2 and 3, the shear force and bending moment at the mud line split significantly into two groups, as does the axial force in the central member and the lower brace (see Table 4).

Location	Axial Force									Spread Euler-Bernoulli	Spread Timoshenko	Overall Spread
	CWMT	CWMT	CWMT	GH	GH	LUH	Risoe	Risoe	SWE			
	ADCoS	ANSYS Beam	ANSYS Pipe	Bladed	Bladed (Timoshenko)	WaveLoads ANSYS	HAWC2	HAWC2_BE	FLEX5 Poseidon			
1	-7087.10	-7100.70	-7100.70	-7101.00	-7101.00	-7100.69	-7101.87	-7101.87	-7054.62	0.67%	0.02%	0.67%
2	-7223.80	-7237.40	-7237.40	-7237.00	-7237.00	-7237.38	-7238.64	-7238.64	-7191.31	0.65%	0.02%	0.65%
3	432.70	392.00	731.35	422.05	755.80	391.97	736.25	397.38	391.54	10.17%	3.30%	70.49%
4	-3902.70			-3889.00	-4020.00	-3877.73	-4013.30	-3880.68	-3861.51	1.06%	0.17%	4.04%
5	-1107.80			-1127.00	-792.40	-1149.59	-813.63	-1150.95	-1149.84	3.79%	2.64%	34.42%
6	-5028.80	-5027.70	-5027.80	-5028.00	-5028.00	-5027.73	-5031.63	-5031.53	-5013.91	0.35%	0.08%	0.35%

Table 2. Static bending moment at locations 1–6

Location	Shear Force									Spread Euler-Bernoulli	Spread Timoshenko	Overall Spread
	CWMT	CWMT	CWMT	GH	GH	LUH	Risoe	Risoe	SWE			
	ADCoS	ANSYS Beam	ANSYS Pipe	Bladed	Bladed (Timoshenko)	WaveLoads ANSYS	HAWC2	HAWC2_BE	FLEX5 Poseidon			
1												
2												
3	43.33	38.24	37.83	38.03	37.76	38.24	37.72	38.13	38.96	13.53%	0.28%	14.49%
4	37.66			35.97	37.00	35.73	36.93	35.77	35.88	5.34%	0.17%	5.31%
5	58.05			59.28	60.02	54.97	56.98	55.04	54.68	8.15%	5.19%	9.36%
6	-2824.30	-2879.60	-2228.90	-2865.00	-2219.00	-2879.58	-2232.41	-2882.17	-2872.23	2.02%	0.60%	24.99%

Table 3. Static shear force at locations 1–6

Location	Bending moment									Spread Euler-Bernoulli	Spread Timoshenko	Overall Spread
	CWMT	CWMT	CWMT	GH	GH	LUH	Risoe	Risoe	SWE			
	ADCoS	ANSYS Beam	ANSYS Pipe	Bladed	Bladed (Timoshenko)	WaveLoads ANSYS	HAWC2	HAWC2_BE	FLEX5 Poseidon			
1	-1382.00	-1386.60	-1386.60	-1382.00	-1382.00	-1386.65	-1383.07	-1383.07	-1435.49	3.84%	0.33%	3.85%
2	-1382.00	-1386.60	-1386.60	-1382.00	-1382.00	-1386.65	-1383.07	-1383.07	-1435.48	3.84%	0.33%	3.85%
3	-746.29	-814.74	-810.80	-811.86	-811.86	-814.74	-808.41	-812.39	-826.61	9.98%	0.42%	9.96%
4	855.37			870.37	893.03	871.29	894.53	871.67	875.40	2.31%	0.17%	4.47%
5	207.15			232.16	239.50	213.32	226.09	213.39	213.36	11.59%	5.76%	14.66%
6	-9469.80	-8972.90	-7318.20	-8975.00	-7320.00	-8972.86	-7330.73	-8983.10	-8930.95	5.95%	0.17%	25.39%

Table 4. Static axial force at locations 1–6

Overall, the agreement is good, once the beam element formulation is taken into account. Results are typically within a few percentage points of each other, but more when the load is small compared to the loads in surrounding members; for example, the axial force at location 3, the central, tapered member.

B. Load Case 2.6: Regular Waves Acting on a Support Structure Modeled as a Rigid Structure

Overall, the results for bending moment (Figure 9) agree well. Above the waterline (locations 1 and 2) there are offsets, but the amplitude of the change caused by the passing of the wave is similar. There is good agreement in the tapered member (location 3) and in the upwind leg (location 4). By the lower brace and pile (locations 5 and 6), there are variations between the codes caused by different methods of accounting for the overlap and for implementing the beam model.

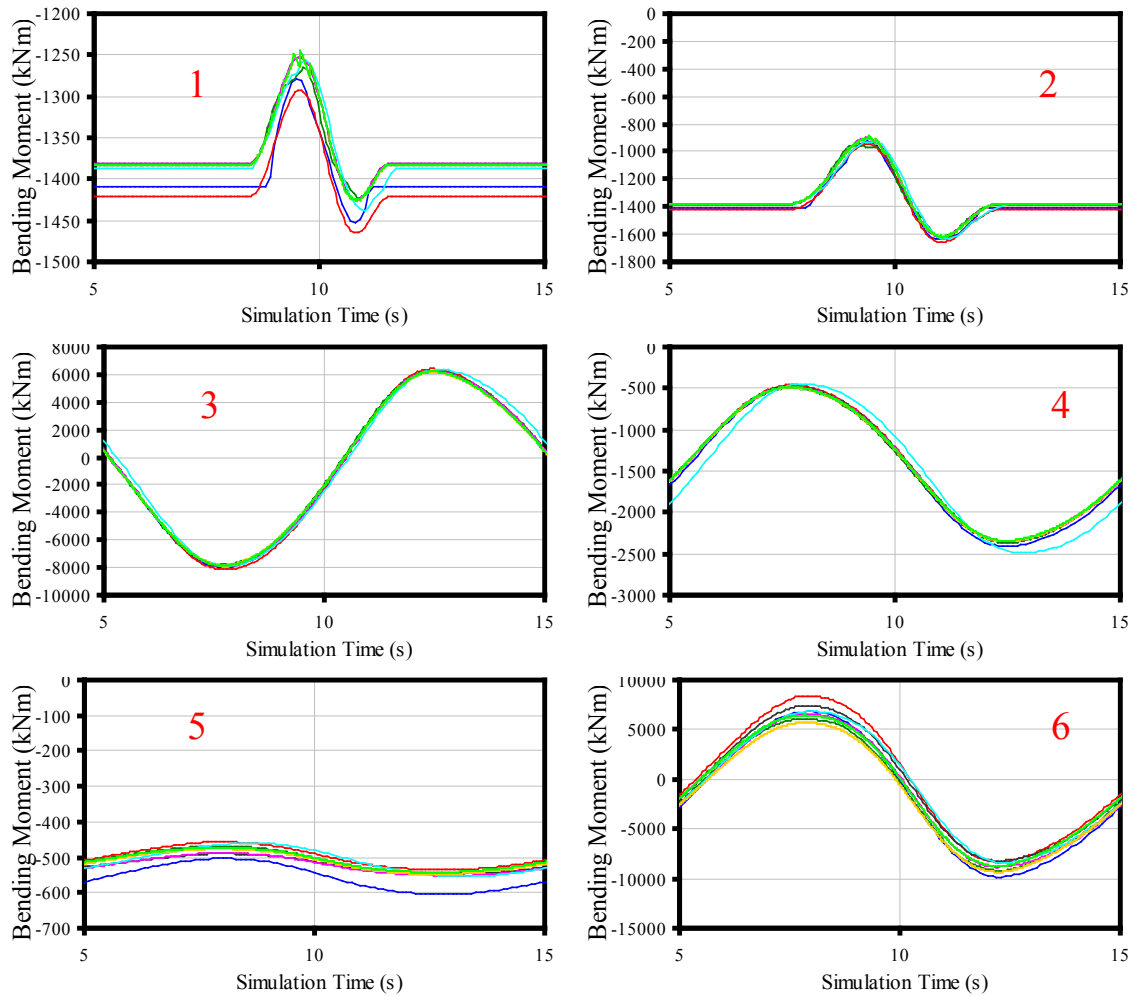


Figure 9. Fore-aft bending moment at locations 1–6

The shear forces agree less well than the bending moments (Figure 10). There are some differences because of the implementation of the wave kinematics. Although a standard set was created, some codes were unable to use this as input. Therefore, there are some differences caused by the wave models used.

The widest variation is seen in the central member (location 3). There are several complications for the calculations of this force: the member is tapered; it is not inside a tree-like structure so there are many paths that the loads can be distributed along; and it is at the height at which the wave loads are strongest. Better agreement is seen in the two braces and at the mudline.

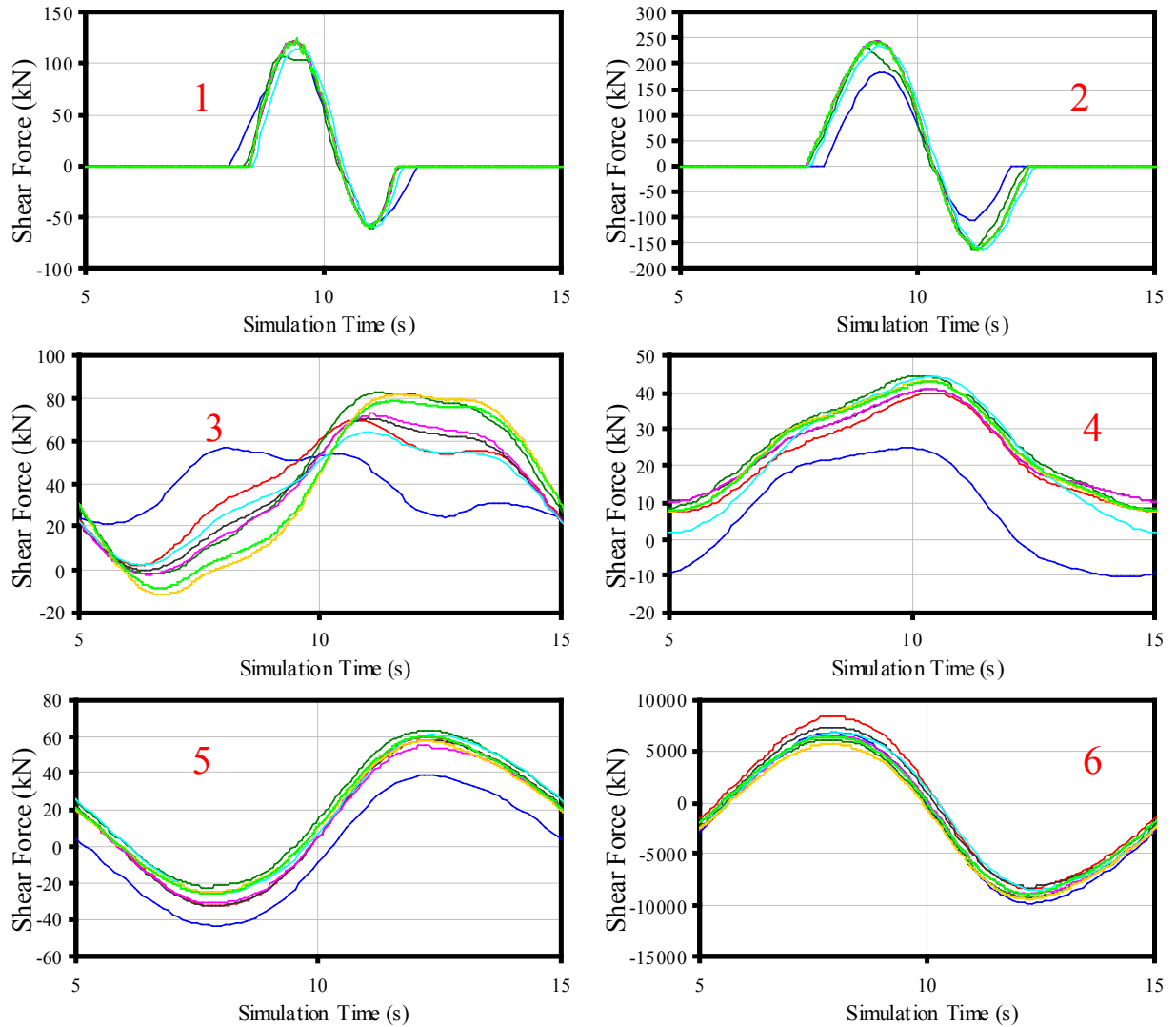


Figure 10. Fore-aft shear force at locations 1–6

Overall, the agreement is good for the axial forces (Figure 11). One difference that can be seen is between the three Bladed simulations. One (in red) has the model strictly defined as in the specification; the others have some parts of the members made invisible to waves and buoyancy to estimate the effect that the members do not overlap. During the course of the project we found that the area of overlap is a relatively large effect for tripod-like structures and should not be ignored.

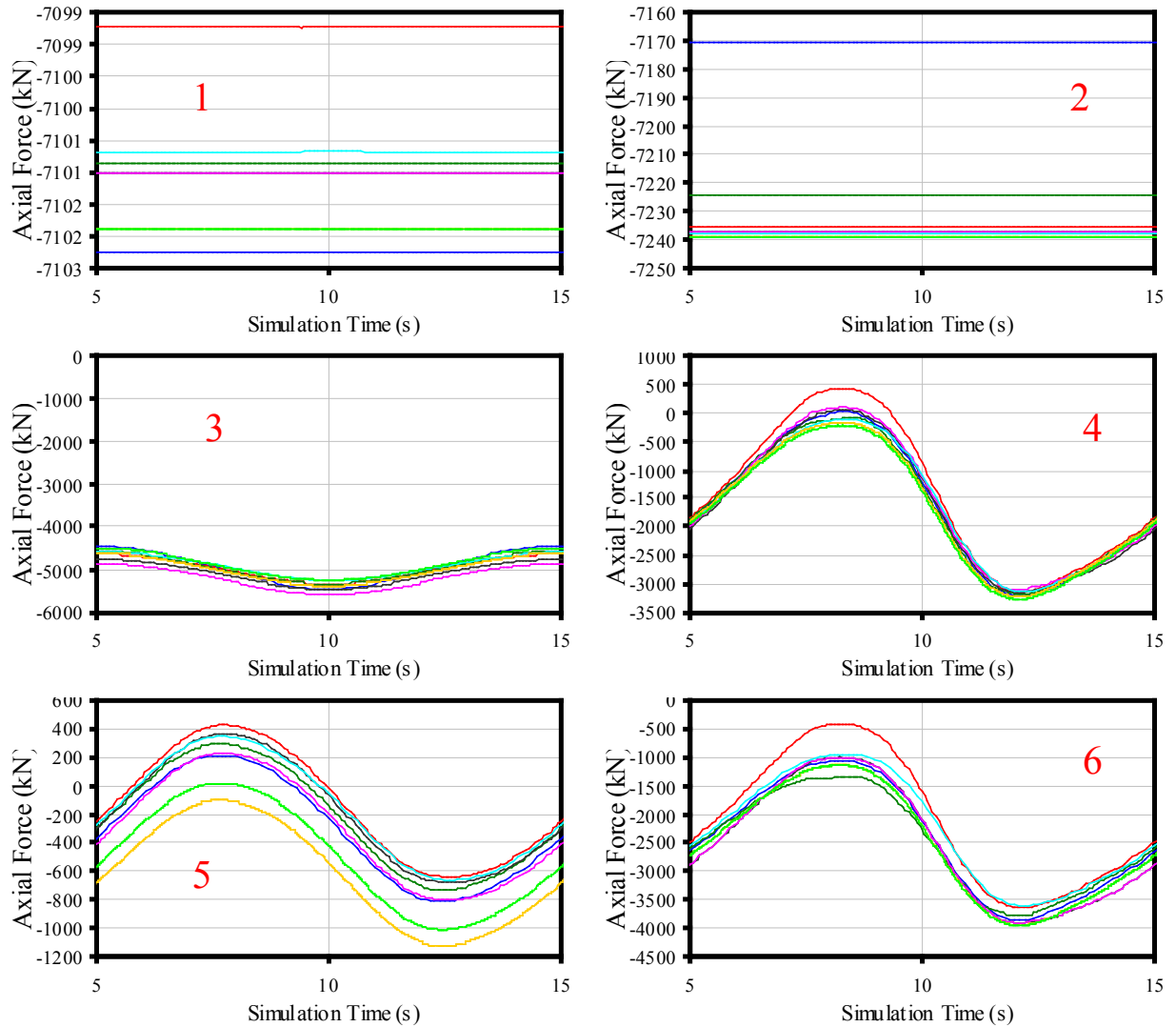


Figure 11. Axial force at locations 1–6

In general the design of the tripod will be determined by the maximum stresses for extreme loads and the cycles of loads for fatigue loads. A comparison of the absolute maximum and range of load for the different codes is shown in Tables 5 and 6. Results are not presented for all codes, as not all of the codes were able to produce full results for each simulation.

Location	Maximum Absolute Bending Moment [kNm]						Spread
	CENER	CENER	GH	Risoe	CWMT	LUH	
	FAST	Bladed	Bladed	HAWC2	ADCoS	WaveLoads ANSYS	
1	1452.57	1465.27	1426.00	1537.84	1423.00	1437.86	7.88%
2	1638.13	1659.97	1621.00	1739.21	1639.00	1638.33	7.14%
3	7975.49	8143.26	7913.00	7888.92	7805.70	7942.55	4.25%
4	2413.70	2349.06	2354.00	2354.08	2367.00	2490.04	5.90%
5	604.25	534.93	545.96	548.24	545.86	553.61	12.48%
6	9829.42	8393.65	8201.00	9362.83	9210.20	8414.37	18.29%

Table 5. Maximum bending moment at locations 1–6

Location	Bending Moment Range [kNm]						Spread
	CENER	CENER	GH	Risoe	CWMT	LUH	
	FAST	Bladed	Bladed	HAWC2	ADCoS	WaveLoads ANSYS	
1	174.18	171.90	173.00	181.20	158.30	180.98	13.22%
2	710.74	712.26	716.04	737.70	684.36	706.22	7.50%
3	14252.62	14549.55	14149.00	13978.36	14081.80	14277.51	4.02%
4	1925.56	1889.33	1877.89	1860.78	1872.07	2042.09	9.49%
5	100.44	78.15	55.86	71.95	76.88	93.28	56.13%
6	16647.57	16746.48	15583.00	15064.66	15297.70	15229.90	10.67%

Table 6. Bending moment range at locations 1–6

C. Load Case 4.3: Regular Waves Acting on a Flexible Support Structure (Rigid Rotor and No Aerodynamics)

Figure 12 shows that the tower top displacement is relatively similar in character, but that there is a fairly wide variation in the phase of the motion between the codes. This could be due to the initial conditions that are used for the simulation.

The mean sea level displacement (see Figures 13 and 14) shows much better agreement. In this case, most of the motion is dominated by the action of the waves.

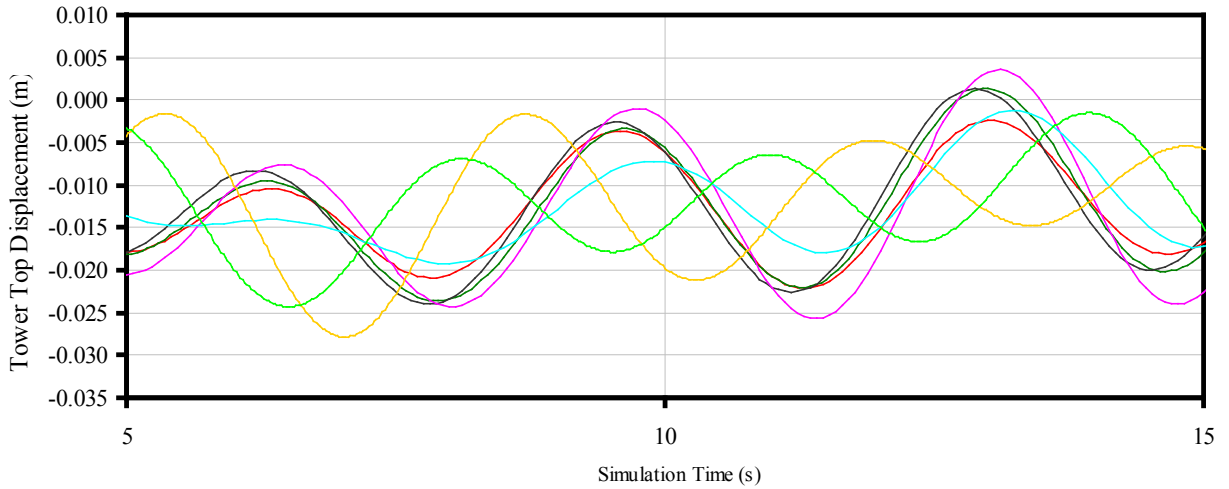


Figure 12. Tower top fore-aft displacement

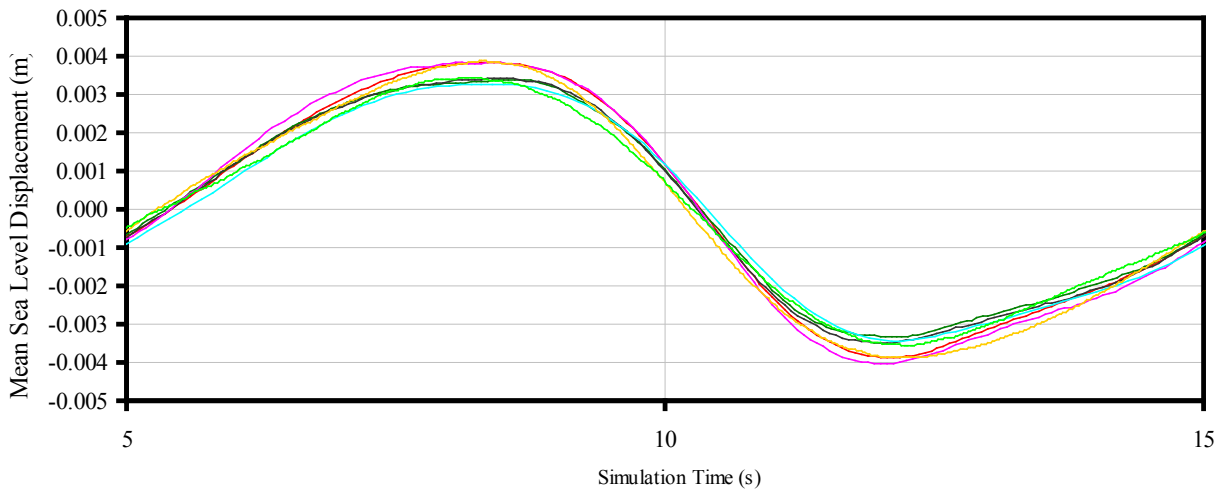


Figure 13. Mean sea level fore-aft displacement

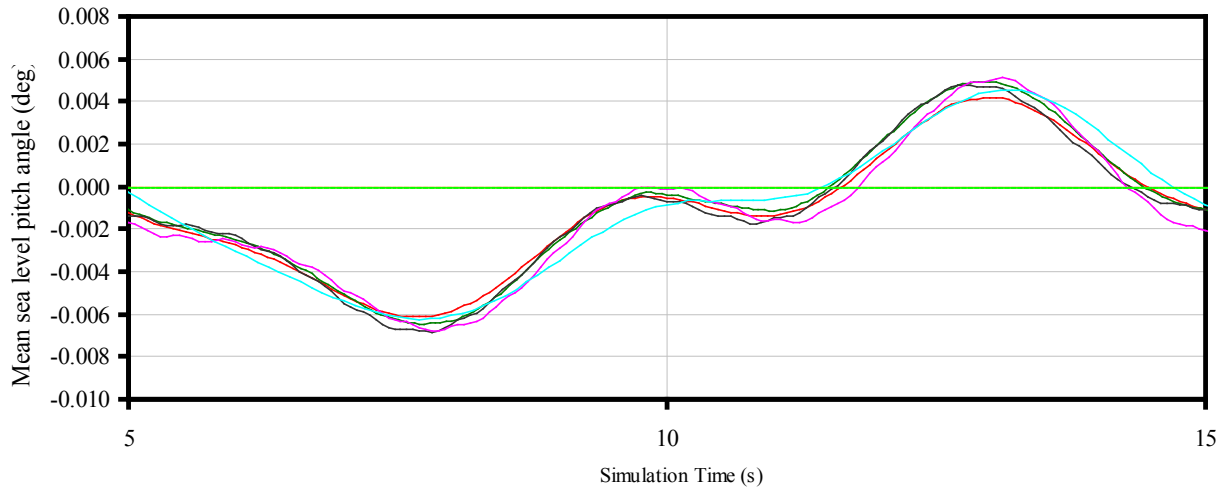


Figure 14. Mean sea level fore-aft pitch angle

To show how important the consideration of dynamics is to the loading on the tower, the differences in maximum bending moment and bending moment range between load cases 2.6 and 4.3 are presented in Tables 7 and 8.

Location	Bending Moment Range [kNm]							
	CENER	CENER	CWMT	GH	GH	LUH	Risoe	Risoe
	FAST NASTRAN	Bladed	ADCoS	Bladed	Bladed (Timoshenko)	WaveLoads ANSYS	HAWC2	HAWC2_BE
1	115.12%	87.01%	114.50%	118.02%	173.28%	106.53%	149.46%	123.18%
2	93.36%	78.46%	102.18%	105.86%	151.14%	88.87%	129.51%	98.00%
3	-31.36%	9.17%	12.31%	12.55%	19.04%	11.83%	15.97%	-4.33%
4	-1.07%	0.63%	0.96%	0.93%	1.23%	0.85%	1.29%	0.44%
5	0.79%	-0.02%	0.05%	0.32%	0.20%	-0.26%	0.28%	0.74%
6	0.61%	-0.24%	0.23%	0.09%	0.55%	0.19%	-1.44%	-0.90%

Table 7. Increase in maximum bending moment taking dynamics into account

Location	Bending moment range [kNm]							
	CENER	CENER	CWMT	GH	GH	LUH	Risoe	Risoe
	FAST NASTRAN	Bladed	ADCoS	Bladed	Bladed (Timoshenko)	WaveLoads ANSYS	HAWC2	HAWC2_BE
1	1658.89%	1499.32%	2100.49%	1968.61%	2919.08%	1709.17%	3310.23%	1701.81%
2	343.06%	370.64%	498.80%	488.67%	712.80%	435.99%	788.80%	349.34%
3	-50.27%	9.39%	13.63%	13.61%	19.53%	12.28%	5.40%	0.45%
4	-41.46%	1.75%	2.48%	2.45%	3.56%	2.17%	1.18%	0.02%
5	-30.18%	-1.70%	-2.29%	9.55%	3.89%	2.73%	10.96%	17.41%
6	-40.14%	-0.17%	-0.26%	-0.24%	-0.10%	-0.10%	-1.10%	-0.04%

Table 8. Increase in bending moment range taking dynamics into account

V. Conclusion

Engineers from six institutions, including universities and private companies, participated in Phase III of the OC3 by submitting results. Many more institutions, including those with a background in traditionally offshore industries such as oil and gas, as well as those previously involved in onshore wind energy, have been involved in discussing and analyzing these results.

In learning from the previous phases of the project, the modeling of an onshore turbine and an offshore turbine mounted on a monopile foundation including various models of the soil interaction, the modeling issues that specifically affect the modeling of tripod, and by extension, other space frame substructures, have been exposed. These include:

The sensitivity of wave loads and loads on tapered members to the discretization of the structure.

The proportion of the structure that is double counted if the overlapping sections are not analyzed fully.

The shear deflection of the members, which is not an important effect in a monopile, becomes important when the relative displacements of different sections of the support structure affect the distribution of load.

By examining these modeling differences, progress has been made in knowledge of the best way to use existing codes to produce accurate models as well as in modifying existing codes to include effects that were previously thought to be of only minor influence. The most important result of the analysis is that a Bernoulli-Euler beam element is not sufficient for modeling tripod structures as the shear effect included in the Timoshenko formulation is of utmost importance. For some beam members, the difference in load can be up to a factor of 1.9.

In addition, a baseline set of calculations has been formulated against which new offshore wind turbine codes can be tested. These calculations can also be used to train engineers and promote a rigorous approach to modeling new structures.

A final, fourth phase to the project is underway, focusing on a floating “spar-buoy” structure supporting the same 5-MW wind turbine as the other three phases. As well as attracting involvement from more parties, this stage of the project is expected to stretch the modeling capabilities of existing codes as nonlinear effects caused by the large motion of a floating structure become important.

References

- ¹ Passon P and Kühn M, “State-of-the-art and Development Needs of Simulation Codes for Offshore Wind Turbines,” Copenhagen Offshore Wind 2005 Conference and Expedition Proceedings, 26–28 October 2005, Copenhagen, Denmark [CD-ROM], Copenhagen, Denmark: Danish Wind Energy Association, October 2005.
- ² Jonkman J, Butterfield S, Musial W, and Scott G, Definition of a 5-MW Reference Wind Turbine for Offshore System Development, NREL/TP-500-38060, Golden, CO: National Renewable Energy Laboratory, February 2007 (to be published).
- ³ Passon P, Kühn M, Butterfield S, Jonkman J, Camp T, and Larsen TJ, “OC3—Benchmark Exercise of Aero-Elastic Offshore Wind Turbine Codes,” Journal of Physics: Conference Series, The Second Conference on The Science of Making Torque From Wind, Copenhagen, Denmark, 28–31 August 2007, [online journal], Vol. 75, 2007, 012071, URL: http://www.iop.org/EJ/article/1742-6596/75/1/012071/jpconf7_75_012071.pdf?request-id=8k111g5u3BGgUobT2wi7Kg, [cited 28 August 2007].
- ⁴ Jonkman J, Butterfield, S Passon P, Larsen T. Camp T, Nichols J, Azcona J, and Martinez A, “Offshore Code Comparison Collaboration within IEA Wind Annex XXIII: Phase II Results Regarding Monopile Foundation Modeling,” 2007 European Offshore Wind Conference.
- ⁵ Guyan RJ, Reduction of Stiffness and Mass Matrices, AIAA Journal, Vol. 3, No. 2, 1965.

REPORT DOCUMENTATION PAGE

Form Approved
OMB No. 0704-0188

The public reporting burden for this collection of information is estimated to average 1 hour per response, including the time for reviewing instructions, searching existing data sources, gathering and maintaining the data needed, and completing and reviewing the collection of information. Send comments regarding this burden estimate or any other aspect of this collection of information, including suggestions for reducing the burden, to Department of Defense, Executive Services and Communications Directorate (0704-0188). Respondents should be aware that notwithstanding any other provision of law, no person shall be subject to any penalty for failing to comply with a collection of information if it does not display a currently valid OMB control number.

PLEASE DO NOT RETURN YOUR FORM TO THE ABOVE ORGANIZATION.

1. REPORT DATE (DD-MM-YYYY) January 2009			2. REPORT TYPE conference paper			3. DATES COVERED (From - To) Jan. 5 - 8, 2009		
4. TITLE AND SUBTITLE Offshore Code Comparison Collaboration within IEA Wind Annex XXIII: Phase III Results Regarding Tripod Support Structure Modeling					5a. CONTRACT NUMBER DE-AC36-08-GO28308			
					5b. GRANT NUMBER			
					5c. PROGRAM ELEMENT NUMBER			
6. AUTHOR(S) Jonkman, J.; Butterfield, S.; Nichols, J.; Camp, T.; Larsen, T.; Hansen, A.; Azcona, J.; Martinez, A.; Munduate, X.; Vorpahl, F.; Kleinhansl, M.; Kohlmeier, M.; Klossel, T.; Boker, C.					5d. PROJECT NUMBER NREL/CP-500-44810			
					5e. TASK NUMBER WER9.4001			
					5f. WORK UNIT NUMBER			
7. PERFORMING ORGANIZATION NAME(S) AND ADDRESS(ES) National Renewable Energy Laboratory 1617 Cole Blvd. Golden, CO 80401-3393					8. PERFORMING ORGANIZATION REPORT NUMBER NREL/CP-500-44810			
9. SPONSORING/MONITORING AGENCY NAME(S) AND ADDRESS(ES)					10. SPONSOR/MONITOR'S ACRONYM(S) NREL			
					11. SPONSORING/MONITORING AGENCY REPORT NUMBER			
12. DISTRIBUTION AVAILABILITY STATEMENT National Technical Information Service U.S. Department of Commerce 5285 Port Royal Road Springfield, VA 22161								
13. SUPPLEMENTARY NOTES								
14. ABSTRACT (Maximum 200 Words) Offshore wind turbines are designed and analyzed using comprehensive simulation codes that account for the coupled dynamics of the wind inflow, aerodynamics, elasticity, and controls of the wind turbine, along with the incident waves, sea current, hydrodynamics, and foundation dynamics of the support structure. This paper presents an overview and describes the latest findings of the code-to-code verification activities of the Offshore Code Comparison Collaboration, which operates under Subtask 2 of the International Energy Agency Wind Annex XXIII. In the latest phase of the project, a variety of project participants used an assortment of codes to model the coupled dynamic response of a 5-MW wind turbine installed on a tripod substructure in 45 m of water. The code predictions from a set of load case simulations—each selected to test different features of the models—were compared side by side. The comparisons have resulted in a more thorough understanding of the modeling techniques and better knowledge of when various approximations are not valid. Importantly, the lessons learned from this exercise have been used to improve the codes of the participants, hence improving the standard of offshore wind turbine modeling.								
15. SUBJECT TERMS wind turbine design codes; offshore wind development; wind energy; wind turbine aerodynamics								
16. SECURITY CLASSIFICATION OF:			17. LIMITATION OF ABSTRACT UL	18. NUMBER OF PAGES	19a. NAME OF RESPONSIBLE PERSON			
a. REPORT Unclassified	b. ABSTRACT Unclassified	c. THIS PAGE Unclassified			19b. TELEPHONE NUMBER (Include area code)			